Immunity, Vol. 22, 385–396, March, 2005, Copyright ©2005 by Elsevier Inc. DOI 10.1016/j.immuni.2005.01.015

Defective Central Tolerance Induction in NOD Mice: Genomics and Genetics

Silvia Zucchelli,[1,2,3] Phil Holler,[1,2] Tetsuya Yamagata,[1,2] Matthew Roy,[1] Christophe Benoist,[1,*] and Diane Mathis[1,*]
[1]Section on Immunology and Immunogenetics
Joslin Diabetes Center
Department of Medicine
Brigham and Women's Hospital
Harvard Medical School
Boston, Massachusetts 02215

Summary

The genetic determinism of type-1 diabetes in NOD mice likely involves complementary defects in central T cell tolerance induction and peripheral immunoregulation. To study the contribution of the NOD genetic background to central tolerance, we followed the behavior of BDC2.5 clonotype thymocytes in fetal thymic organ cultures (FTOC). The NOD genetic background encodes a quantitative deficiency in the ability to delete these self-reactive thymocytes and to divert them to the CD8αα lineage. In genetic analyses, comparing NOD and B6.*H2*^{g7} FTOCs, the NOD defect incorporated the influence of several loci (notably ones on *chr1* and *3*). Microarray analyses assessing FTOCs from the same two strains argued that the NOD abnormality reflects the combined effects of turning down the gene expression program that provokes apoptosis and turning on a new program promoting cell survival. Intersection of the data from the two approaches points to a small set of attractive candidate genes.

Introduction

The induction of T lymphocyte tolerance has two major facets: peripheral tolerance, wherein regulatory genes or cells dampen mature T cell activation or effector function; and central tolerance, in which potentially autoreactive T cells are eliminated or silenced at an immature stage of differentiation in the thymus. The most definitive mechanism of central tolerance induction is the clonal deletion of self-reactive thymocytes (reviewed in Starr et al., 2003). Apoptosis of recalcitrant T cell precursors occurs when their T cell receptors (TCRs) are engaged with high affinity by major histocompatibility complex (MHC) molecule/self-Ag complexes encountered on thymic stromal cells. The apoptotic pathways involved remain ill defined, but several critical molecular players have been identified: Nur77, a transcription factor, and related family members (Woronicz et al., 1994; Calnan et al., 1995); members of the Bcl2 family of apoptosis control factors, Bim, Bak, and Bax (Rathmell et al., 2002; Bouillet et al., 2002); and NF-κB pathway regulators, in particular IκBNS (Fiorini et al., 2002). Roles for TNF:TNF receptor family members like Fas-Fas ligand have also been proposed, but these are more controversial. Depending on several parameters, the engagement of TCRs on differentiating thymocytes by agonist ligands can also promote, rather than delete, their diversion to alternative cell fates, e.g., selection of T cells expressing the CD8αα coreceptor and displaying innate immune system characteristics (Leishman et al., 2002; Yamagata et al., 2004) or of CD4$^+$CD25$^+$ T cells with regulatory properties (Jordan et al., 2001; Apostolou et al., 2002; Yamashiro et al., 2002).

It has been hypothesized that ineffective central tolerance induction in NOD mice, the reference mouse model of autoimmune diabetes, is an important, though not the sole, contributor to their propensity to autoimmunity. Experimental support for this notion has recently been provided by two approaches. First, abnormal clonal deletion of NOD thymocytes after engagement of TCRs by systemic injection of anti-CD3 mAb or of superantigen was reported (Kishimoto and Sprent, 2001), although this result was later challenged (Villunger et al., 2003). Second, coupling of a TCR transgenic (tg) mouse line with a second tg line expressing the cognate neo-Ag in the thymus led to drastically reduced maturation of CD4$^+$ cells, but this reduction was much milder in NOD-background mice (Lesage et al., 2002). The NOD deficiencies in clonal deletion were specified by non-MHC genes. Interestingly, it has been proposed that human diabetic patients may have defective clonal deletion of thymocytes reactive to insulin. This defect is linked to sequence polymorphisms in the *INS* promoter that may reduce its expression in the thymus (reviewed in Pugliese and Miceli, 2002), a proposition consistent with recent results on *ins* gene knockout mice (Thebault-Baumont et al., 2003).

The NOD mouse is an invaluable experimental tool, but diabetogenesis is exceedingly complex even in this model, with multiple and complex genetic and environmental influences. Thus, a number of investigators have preferred to focus their efforts on dissecting disease subphenotypes. One such strategy has been to employ TCR tg lines that carry the rearranged TCR genes from a diabetogenic T cell clone, which allow one to conveniently track the life history of autoreactive T lymphocytes. The BDC2.5 line derives from a CD4$^+$ T cell clone, restricted by the NOD MHC class II A^{g7} molecule and specific for an unknown β cell protein (Katz et al., 1993; Bergman and Haskins, 1994). This line has been instrumental in the elucidation of several features of the immunoregulatory genes or cells that control the aggressivity of autoreactive T cells in the periphery (Gonzalez et al., 1997; Kanagawa et al., 2002; Poirot et al., 2004). Here, we have analyzed the impact of NOD-background genes on the negative selection of immature T cells expressing the BDC2.5 clonotype.

*Correspondence: cbdm@joslin.harvard.edu (C.B. and D.M.)
[2]These authors contributed equally to this work.
[3]Present address: SISSA-LNM Area Science Park, Padriciano 99, 34012 Trieste, Italy.

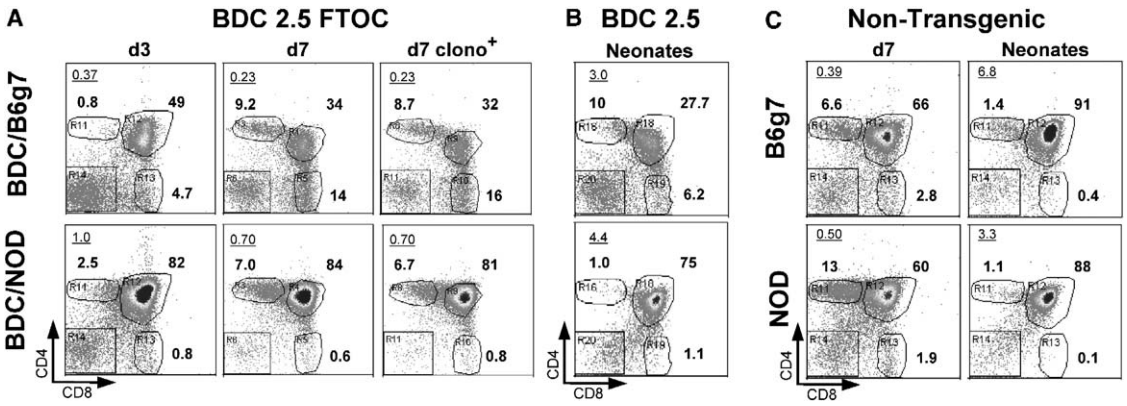

Figure 1. The NOD Background Prevents Clonal Deletion of BDC2.5 T Cells by Autoantigen

(A) BDC2.5-tg FTOCs were cultured for 3 or 7 days before analysis by flow cytometry. Right panels are gated for the BDC2.5 clonotype. The bold numbers show the proportion of cells in the populations, and the underlined numbers show the total cell yield per lobe (representative of three or more experiments).

(B) Thymic lobes from newborn mice of the same transgenic lines were analyzed as described in (A).

(C) No difference in clonal deletion in nontransgenic FTOCs (left) or neonates (right).

Results

Defective Clonal Deletion in Fetal and Neonatal BDC2.5/NOD Thymi

For focus and flexibility, we chose to investigate T lymphocyte central tolerance induction in NOD mice by using FTOCs. The behavior of thymocytes displaying the BDC2.5 clonotype afforded a convenient and sensitive readout. FTOCs derived from congenic BDC2.5 TCR tg mice of the NOD and C57Bl/6.*H2*^{g7} (B6g7) genetic backgrounds were compared, permitting a straightforward assessment of influences by non-MHC genetic loci. This strain combination was particularly suited to our needs because a library of Single Nucleotide Polymorphisms (SNPs) distinguishing the NOD and B6 strains has already been established, and because genetic intervals associated with strain-dependent differences in diabetes susceptibility (*Idds*) have been defined.

Thymic lobes dissected from day 15.5 embryos derived from parallel matings of the BDC2.5/NOD and BDC2.5/B6g7 lines were cultured as FTOCs for 3–7 days, and the resulting thymocytes were analyzed for CD4/CD8 profiles by flow cytometry (Figure 1A, left and center panels). Lobes from the BDC2.5/NOD cultures looked quite normal in their high proportion of immature double-positive (DP) thymocytes and predominant selection into the CD4-single-positive (CD4-SP) mature T cell compartment. In contrast, the BDC2.5/B6g7 lobes showed clear hallmarks of clonal deletion: reduced total thymocyte numbers; a low proportion of DPs, showing reduced expression of CD4; fewer CD4-SPs; and an increased proportion of CD8-SPs. These differences persisted when CD4/CD8 profiles of cells gated as expressing the BDC2.5 clonotype were plotted (Figure 1A, right panels).

We then asked whether the deletion-resistant phenotype found for BDC2.5/NOD mice was restricted to fetal thymocytes differentiating in an organ culture system or whether the same phenotype could be demonstrated ex vivo. In a previous study (Gonzalez et al., 1997), we found no differences between adult BDC2.5/B6g7 and BDC2.5/NOD thymi, with no overt signs of negative selection on either background. However, it remained possible that cues for or mechanisms of clonal deletion might be developmentally regulated, so we analyzed the phenotype of BDC2.5/NOD and BDC2.5/B6g7 mice at late (d18–19) embryonic (not shown) and postnatal (Figure 1B) stages. Thymi from neonates exhibited phenotypes that paralleled those observed in FTOCs: a normal aspect in BDC2.5/NOD thymi, contrasting with a clear imprint of negative selection in BDC2.5/B6g7 thymi, with as low as 28% DP thymocytes.

Thus, the NOD genetic background appeared to confer resistance to clonal deletion in differentiating thymocytes that express the BDC2.5 specificity. Non-tg littermates were analyzed in order to confirm that the different profiles resulted from specific deletion of cells expressing the self-reactive clonotype, rather than from a differential susceptibility of embryonic thymi of the NOD versus B6.*H2*^{g7} genetic background to the culture conditions. FTOCs and neonatal thymic lobes from both genetic backgrounds showed a normal representation of thymocyte compartments, in particular healthy DP compartments (Figure 1C). A difference in the CD4/CD8 ratios was observed, consistent with the generally higher proportion of CD4$^+$ cells in the NOD mouse (Zhang et al., 1994).

Clonal deletion of thymocytes expressing the BDC2.5 clonotype observed in FTOCs likely reflects ectopic expression in thymic epithelial cells (Kyewski et al., 2002) of low amounts of the BDC2.5 autoAg; this molecule's expression appears otherwise to be restricted to the pancreas (Bergman and Haskins, 1994). It is conceivable that BDC2.5/B6g7 FTOCs express more of the BDC2.5 autoAg than do BDC2.5/NOD cultures, thereby providing an explanation of the above results. To evalu-

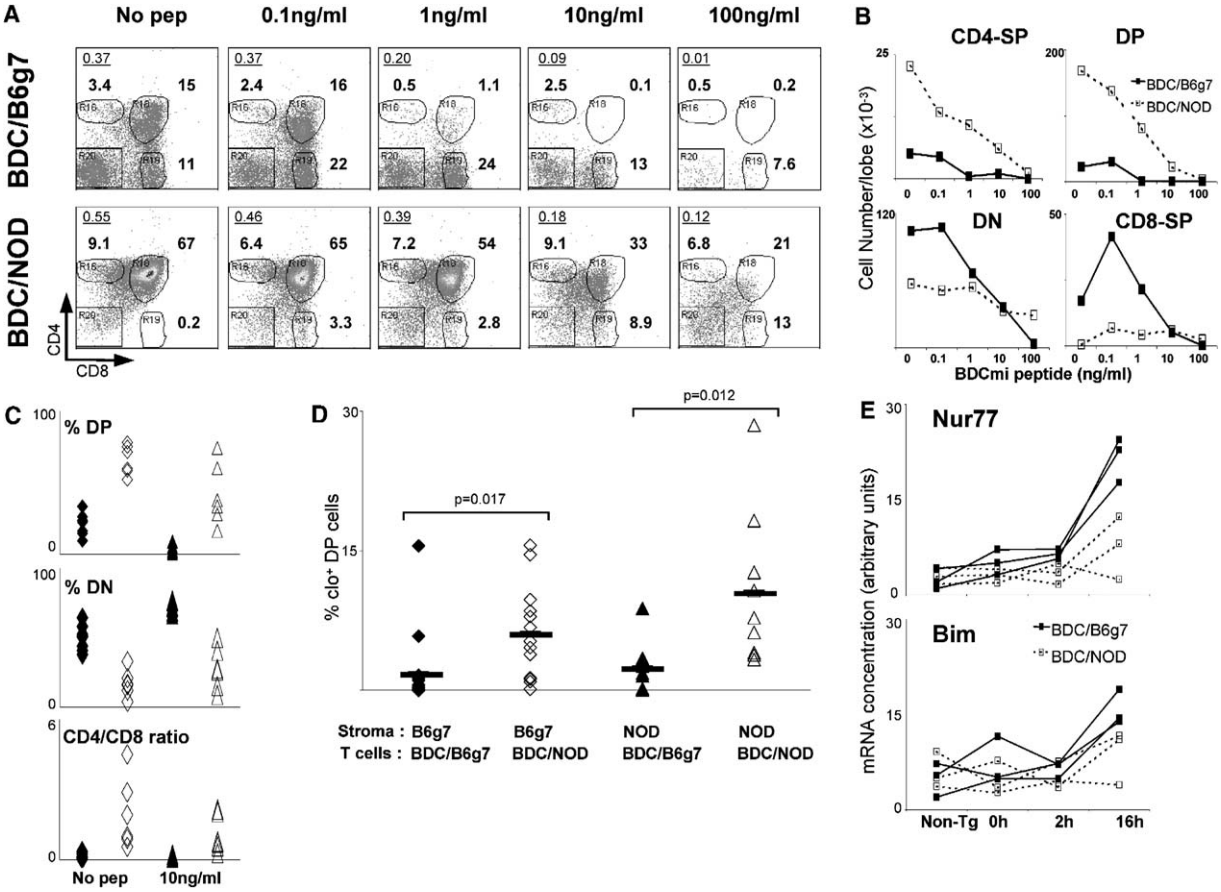

Figure 2. Decreased Sensitivity of NOD Background Thymocytes to Peptide-Induced Deletion

(A) BDC2.5-tg FTOCs were cultured for 7 days with graded doses of BDCmi and were analyzed by flow cytometry (representative of more than five experiments).

(B) Absolute cell counts per lobe from the experiment shown in (A).

(C) Differences among groups of BDC2.5/B6g7 (black symbols) or BDC2.5/NOD (white symbols) cultures; each point represents an FTOC lobe.

(D) Reconstitute FTOCs were assembled by mixing sorted T precursors and deoxyguanosine-treated stromal cells and were evaluated by flow cytometry.

(E) Induction of proapoptotic molecules, as measured by RT-PCR in peptide-stimulated sorted DP FTOC cells.

ate this possibility, and to provide more quantitative control of the level of autoAg, we performed FTOC experiments in the presence of graded amounts of a mimotope peptide that activates mature BDC2.5 T cells (BDCmi; [Judkowski et al., 2001]). In keeping with the results obtained on untreated cultures, BDC2.5/B6g7 lobes exhibited a much greater sensitivity to this agonist than did the BDC2.5/NOD lobes cultured in parallel (Figures 2A–2C). In BDC2.5/B6g7 thymi, DP cells were essentially wiped out by the addition of 1 ng/ml peptide, leaving behind only a few double-negative (DN) precursors and CD8-SP cells; the same dose had little effect on BDC2.5/NOD lobes, which required up to 100 ng/ml peptide for a comparable degree of depletion. Thus, the different outcomes of the BDC2.5/NOD and BDC2.5/B6g7 FTOCs appeared to reflect a 50- to 100-fold difference in sensitivity to clonal deletion, not in the expression level of autoAg.

The inefficient deletion of self-reactive thymocytes on the NOD genetic background could stem from either altered autoAg presentation by thymic stromal cells or from an autonomous defect in the response elicited in immature T cells. To distinguish between these two possibilities, we constructed chimeric fetal thymus lobes (Figure 2D): stromal cells from deoxyguanosine-treated E15 lobes were reconstituted with sorted DN T cell precursors (depleted of CD11c$^+$, CD11b$^+$, MHC class II$^+$ antigen presenting cells [APCs]) in all four possible combinations of genetic background. Independent of whether the stromal cells were of NOD or B6g7 origin, seeding with BDC2.5/B6g7 T cell precursors recapitulated the deletion-sensitive phenotype (low % DP cells), while introducing BDC2.5/NOD T precursors yielded cultures that were significantly more resistant to deletion. Thus, the impaired ability to delete BDC2.5 T cells in thymi of NOD mice resides with the thymocytes themselves, consistent with observations on the TCR/neo-self-Ag double-tg system mentioned above (Lesage et al., 2002).

One might predict that this greater propensity to die

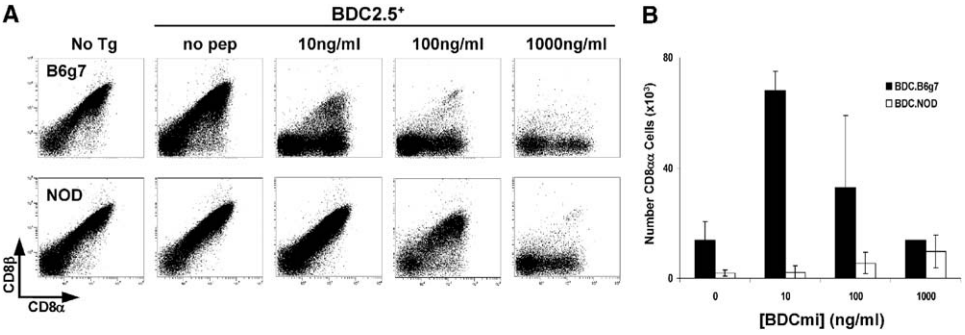

Figure 3. Defective Commitment to the CD8αα+ Lineage in Agonist-Stimulated NOD Thymocytes

(A) BDC2.5-tg FTOCs were cultured for 7 days with graded amounts of BDCmi and were analyzed by flow cytometry (gated on total thymocytes).

(B) Absolute numbers of CD8αα thymocytes obtained from BDC2.5-tg FTOCs, ±SD.

would be reflected in a differential balance of pro- and antiapoptotic mediators. We tested the induction of two such elements, known to be essential in thymic clonal deletion, Nur77 and Bim (Calnan et al., 1995; Bouillet et al., 2002). As illustrated in Figure 2E, both were induced at higher levels in BDC2.5/B6g7 than in BDC2.5/NOD DP cells by peptide addition.

Compromised Diversion to the CD8αα Lineage in NOD-Background FTOCs

While strong agonist ligand engagement of TCRs in the thymus has classically been linked to clonal deletion, recent studies have demonstrated that it can also elicit differentiation along alternative pathways, such as the CD8αα lineage (Leishman et al., 2002; Yamagata et al., 2004). Having established that the efficiency of thymocyte clonal deletion differs between BDC2.5/NOD and BDC2.5/B6g7 thymi, we exploited our FTOC system to determine whether thymi of the two strains also diverge in their ability to redirect self-reactive thymocytes into the CD8αα lineage. BDC2.5/B6g7 FTOCs contained significant numbers of CD8αα thymocytes, and the ratio of CD8αα to CD8αβ cells increased with mimotope peptide dose, ultimately resulting in nearly complete "conversion" to CD8αα cells at high peptide concentrations (Figure 3A, top panels). In contrast, BDC2.5/NOD FTOCs yielded CD8αα thymocytes only in the presence of 30- to 100-fold higher BDCmi concentrations (Figure 3A, bottom panels), a shift similar to that found for the deletion curves of DP and CD4-SP cells (Figures 2A and 2B). Furthermore, in BDC2.5/NOD FTOCs, as peptide concentration was increased, depletion of the general population of CD8-SP cells preceded the increase in the CD8αα component. This trend, combined with the consistently lower numbers of CD8-SPs observed in BDC2.5/NOD cultures, resulted in far lower yields of CD8αα cells at all but the highest concentrations (Figure 3B). Thus, a failure to "disarm" self-reactive T cells by diverting them to an alternative lineage accompanies the deficiency in clonal deletion characteristic of NOD thymocytes.

Broad Differences in Gene Expression Profiles

What changes in gene expression underlie the differential sensitivity to clonal deletion of the BDC2.5 clonotype on the NOD versus B6g7 genetic backgrounds? Our initial analyses showed a stronger induction of proapoptotic molecules on the B6g7 background; but, for a broad perspective on this question, we performed microarray analysis on thymocytes of FTOCs derived from BDC2.5/NOD and BDC2.5/B6g7 embryos and cultured in the presence of BDCmi peptide subsequent to day 3. The lobes were dissociated 0, 2, or 16 hr after peptide addition in order to span the initiation of apoptosis; thymocytes remained fully viable at those times, beginning to disappear only 24 hr after peptide addition (data not shown). DP thymocytes were isolated, and RNA was prepared, amplified, and labeled for hybridization to Mu74Av2 Affymetrix gene chips. Data from three completely independent replicates per condition were processed and normalized as described previously (Yamagata et al., 2004), with estimates of the significance of the variations observed deduced from randomized data sets (full results are shown in Table S1; see the Supplemental Data available online).

Figure 4A portrays the changes in gene expression observed 16 hr after addition of the BDCmi peptide. For both the BDC2.5/NOD and BDC2.5/B6g7 FTOCs, a number of genes depart from the midline of equivalent expression. The blue dots highlight genes demonstrated in studies published by other groups to be induced during negative selection (Schmitz et al., 2003; Huang et al., 2004; DeRyckere et al., 2003). Indeed, most of these previously implicated genes were induced at 16 hr in our system as well, particularly in the BDC2.5/B6g7 cultures, thus instilling confidence that the variations we observed are relevant. For example, transcripts from the *Nur77* gene were found to be strongly induced, more so in BDC2.5/B6g7 than in BDC2.5/NOD FTOCs. A time course analysis (Figure 4B) demonstrates that these genes were only slightly upregulated at 2 hr, but significantly at 16 hr. These trends extended to unexpected genes as well: the *Gadd45b* gene transcript, for instance, displayed the same pattern. In all, 37 and 86 genes were induced or repressed (respectively) more than 2-fold in BDC/B6g7 FTOCs, versus only 14 and 0 (respectively) for BDC2.5/NOD cultures. Thus, although several genes typically induced during negative selection were also upregulated on both the NOD and B6g7 backgrounds, these

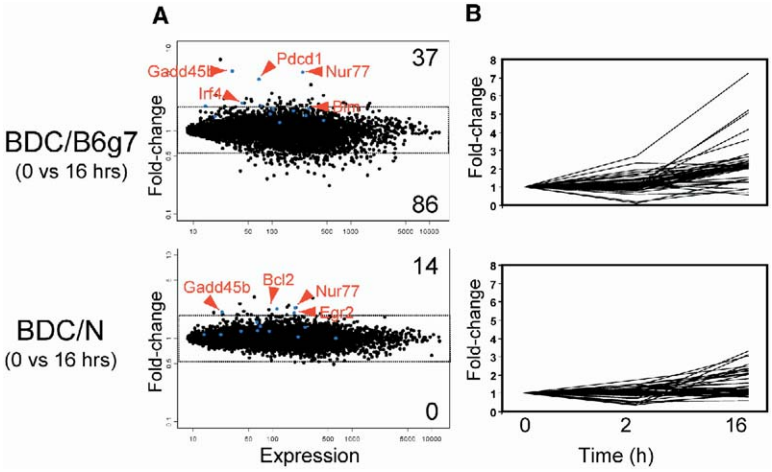

Figure 4. Broad Induction of the Apoptosis-Related Genes in BDC2.5/B6g7 versus BDC2.5/NOD

(A) BDC2.5-tg FTOCs were cultured for 3 days in the absence of peptide followed by peptide challenge. mRNA was harvested from sorted DP thymocytes and hybridized to Mu74Av2 chips. Blue genes exhibited differential expression in previous studies of negative selection. The numbers of genes that are induced or repressed more than 2-fold are shown.

(B) The kinetics of genes induced more than 2-fold for BDC2.5/B6g7 or BDC2.5/NOD.

increases were distinctly less marked on the former, consistent with the resistance of NOD thymi to clonal deletion.

We then analyzed more profoundly the differences observed between the BDC2.5/NOD and BDC2.5/B6g7 expression profiles. In theory, one might have expected two categories of differentially expressed genes, both of which could have a causative relationship with the efficacy of clonal deletion. The first category corresponds to genes whose expression differences are constitutive, i.e., exist prior to and independent of the negative selection trigger. Such genes represent "bedrock" variation between the NOD and B6g7 strains, and a substantial number showed this pattern (Figure S1): with a cutoff of 2.0-fold, 25 and 17 genes were consistently expressed at a higher level in B6g7 and NOD thymocytes, respectively, whether peptide was present or not, and also in cells from non-tg lobes. Most of these differences had also been seen in microarray data sets obtained from lymph node $CD4^+$ T cells of BDC2.5/NOD or BDC2.5/B6g7 mice (data from Poirot et al., 2004).

The second category of differentially expressed genes consists of those that show a difference only subsequent to induction of negative selection by agonist peptide. This pattern of expression might indicate that these genes' responsiveness is intrinsically different or might reflect that they belong to a pathway that is differentially triggered in the two genetic backgrounds. In other words, the muted BDC2.5/NOD profile could simply reflect a duller induction of the same panel of genes or represent the induction of a different gene set. To facilitate visualization of this category, we plotted all of the genes induced after 16 hr of incubation with mimotope peptide in BDC2.5/B6g7 and BDC2.5/NOD lobes in Figures 5A and 5B, respectively. Among those genes upregulated in the BDC2.5/B6g7 FTOCs, only a minority were also induced in the BDC2.5/NOD cultures (16 of 252 genes at a fold-change cutoff of 1.5). Conversely, of the 127 genes induced in BDC2.5/NOD cultures, only 15 were upregulated in BDC/B6g7 FTOCs, while most were uninduced or even slightly repressed. A notable example is the signal for the antiapoptotic gene *bcl2*, which showed a 2.25-fold increase on the NOD background, but not on the B6g7. This sense of distinct sets of induced genes is reinforced by the plot of Figure 5C, which shows, for all genes upregulated on either genetic background, the ratio of inducibility on the B6g7 versus NOD backgrounds (ratio of the 16 hr/0 hr fold-change values). While a main swath of genes has a B6g7/NOD inducibility ratio > 1, another subset is clearly distinguished below the line of equivalence. The nature of the genes specifically induced on the NOD background is intriguing: many of them are interferon inducible or are related to transcriptional/translational control (Figure 5C, right) (further discussed below). Thus, the resistance to agonist-induced apoptosis on the NOD background is marked both by a dampening of the normal response and by the induction of a qualitatively different gene expression program.

Positioning the Causal Genetic Variation

Which, if any, of these gene expression differences might be causal, actually determining protection from clonal deletion on the NOD background? We performed a genetic mapping study to address this question, first testing for phenotypic dominance by flow cytometric analysis of thymocytes derived from F1 (BDC2.5/B6g7 × NOD) FTOCs. F1 thymocytes were as resistant to deletion as NOD thymocytes (if not more so), in either the presence or absence of BDCmi peptide (Figure 6A). Thus, the resistance phenotype characteristic of the NOD mouse is largely dominant.

To map the underlying quantitative trait loci (QTL), and in a variation of the classic F2 intercross mapping strategy, we set up FTOCs from F2 embryos. A total of 306 $BDC2.5^+$ (B6g7 × NOD) F2 cultures were tested in two different cohorts: the first consisted of 123 cultures incubated in the absence of added peptide; the other 183 were incubated in the presence of the BDCmi peptide at 10 ng/ml, a dose chosen because it provokes significant deletion of BDC2.5/B6g7 thymocytes while only marginally affecting BDC2.5/NOD cells. The F2s exhibited a range of phenotypes, skewed toward the NOD phenotype (Figure 6B), consistent with the appar-

A

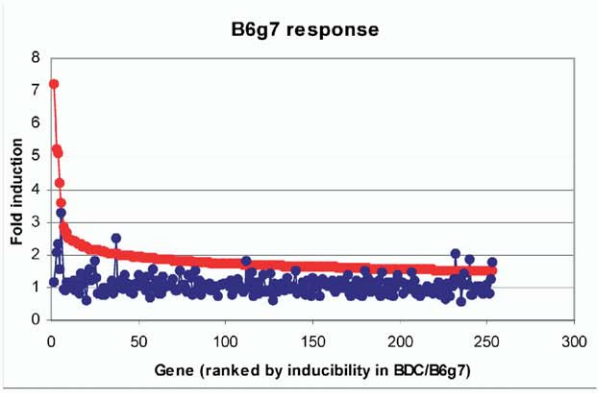

Probe	Title	Symbol	Locus Link	Chr	Mb	B16 / B0	N16 / N0	p-val	FDR
93097_at	arginase 1, liver	Arg1	11846	10	24.6	7.23	1.19	0.237	0.0002
161666_f_	growth arrest and DNA-damage 45b	Gadd45b	17873	10	80.8	5.24	2.06	0.031	0.0002
102371_at	Nur77	Nr4a1	15370	15	101.7	5.09	2.32	0.022	0.0008
98836_at	programmed cell death 1	Pdcd1	18566	1	94.1	4.17	1.56	0.117	0.0008
93511_at	integral membrane protein 2A	Itm2a	16431	99	92.6	3.59	3.30	0.002	0.0008
99096_at	DEAD/H box 13 (RNA helicase A)	Ddx24	27225	12	97.4	2.83	0.94	0.130	0.0030
95053_s_	succinate dehydrogenase, sub B	Sdhb	67680	4	139.1	2.68	0.89	0.221	0.0023
93416_at	TNF superfamily member 11	Tnfsf11	21943	14	68.7	2.68	1.15	0.064	0.0087
96322_at	endothelial differentiation-related factor 1	Edf1	59022	2	25.8	2.51	1.01	0.096	0.0070
160802_a	peter pan homolog (Drosophila)	Ppan	245822	9	20.8	2.45	1.13	0.044	0.0014
95706_at	lectin, galactose binding, soluble 3	Lgals3	16854	14	38.7	2.43	1.15	0.054	0.0034
95673_s_	brain membrane attached signal protein 1	Basp1	70350	15	25.3	2.43	1.19	0.122	0.0107
93918_at	TAF9 RNA pol II, (TBP)-associated factor	Taf9	108143	6	116.3	2.41	0.90	0.992	0.0984
98575_at	fatty acid synthase	Fasn	14104	11	121.7	2.34	1.08	0.077	0.0133
95147_at	6-phosphogluconolactonase	Pgls	66171	8	70.6	2.34	0.81	0.263	0.0133
99109_at	immediate early response 2	Ier2	15936	8	83.9	2.33	1.41	0.096	0.0087
94928_at	TNF receptor superfamily, member 1b	Tnfrsf1b	21938	NA	0.0	2.27	1.07	0.083	0.0043
102914_s	EST	EST	NA	NA	0.0	2.27	1.25	0.130	0.0063
162279_f_	chaperonin subunit 6a (zeta)	Cct6a	12466	NA	0.0	2.23	0.62	0.290	0.0179
93637_at	CD5 antigen	Cd5	12507	19	9.7	2.19	1.31	0.017	0.0087
95034_f_s	importin 4	Ipo4	75751	14	46.3	2.17	1.55	0.011	0.0051
92737_at	interferon regulatory factor 4	Irf4	16364	13	30.2	2.17	1.22	0.098	0.0984
101509_a	von Hippel-Lindau binding protein 1	Vbp1	22327	99	59.7	2.17	1.23	0.992	0.0063
101587_at	epoxide hydrolase 1, microsomal	Ephx1	13849	1	181.7	2.15	1.82	0.039	0.0063
98936_at	seryl-aminoacyl-tRNA synthetase 1	Sars1	20226	3	108.8	2.15	0.81	0.119	0.0087
92775_at	poly A binding protein, cytoplasmic 4	Pabpc4	230721	14	80.5	2.12	0.83	0.054	0.0051
96883_at	eukaryotic translation initiation factor 3, su	Eif3s4	53356	9	20.8	2.10	0.78	0.070	0.0070
100573_f_	glucose phosphate isomerase 1	Gpi1	14751	7	24.0	2.10	1.01	0.175	0.0250
99566_at	triosephosphate isomerase	Tpi	21991	6	125.6	2.10	0.80	0.284	0.0133
101960_at	EST	EST	28088	10	85.5	2.09	0.99	0.154	0.0107
98550_at	SET translocation	Set	56086	1	163.4	2.05	1.01	0.524	0.0359
100578_a	inosine 5'-phosphate dehydrogenase 2	Impdh2	23918	8	99.4	2.05	0.95	0.178	0.0133
94915_at	peptidylprolyl isomerase B	Ppib	19035	9	66.3	2.04	1.20	0.420	0.0179

B

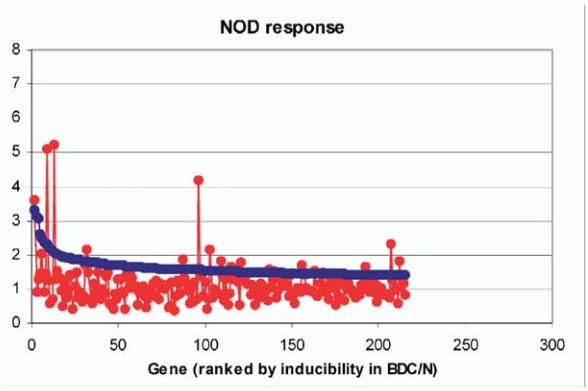

Probe	Title	Symbol	Locus Link	Chr	Mb	B16 / B0	N16 / N0	p-val	FDR
93511_at	integral membrane protein 2A	Itm2a	16431	99	92.6	3.59	3.30	0.029	0.0019
103674_f_	eukaryotic translation initiation factor 2, su	Eif2s3y	26908	NA	0.0	0.90	3.13	0.272	0.0018
102906_at	T-cell specific GTPase	Tgtp	21822	11	49.7	1.30	3.05	0.017	0.0021
103842_at	DEAD box polypeptide, Y chromosome	Dby	26900	NA	0.0	1.44	2.60	0.361	0.0009
160399_r_	H2A histone family, member Y	H2afy	26914	13	55.2	0.90	2.37	0.454	0.0184
161214_r_	hypothetical protein MGC47434	MGC4743	231807	5	135.8	1.44	2.34	0.278	0.0250
102371_at	Nur77	Nr4a1	15370	15	101.7	5.09	2.32	0.054	0.0013
98868_at	B-cell leukemia/lymphoma 2	Bcl2	12043	1	107.0	1.26	2.25	0.007	0.0042
160150_f_	calponin 3, acidic	Cnn3	71994	3	121.9	0.57	2.20	0.035	0.0114
103446_at	RIKEN cDNA 9130009C22 gene	EST	71586	NA	0.0	0.72	2.11	0.066	0.0114
161686_f_	growth arrest and DNA-damage 45b	Gadd45b	17873	10	80.8	5.24	2.06	0.005	0.0057
102736_at	chemokine (C-C motif) ligand 2	Ccl2	20296	11	82.8	1.27	2.04	0.361	0.0250
102661_at	early growth response 2	Egr2	13654	10	67.2	1.52	2.02	0.195	0.0014
161122_f_	---	---	NA	NA	0.0	1.32	1.98	0.299	0.0250
102002_at	ubiquilin 2	Ubqln2	54609	99	133.4	0.97	1.94	0.438	0.0139
94395_at	DNA segment, Chr 3, ERATO Doi 330, exp	EST	51886	3	152.9	0.51	1.94	0.683	0.0385
104096_at	origin recognition complex, subunit 4-like (	Orc4l	26428	2	49.7	1.22	1.94	0.647	0.0385
98030_at	tripartite motif protein 30	Trim30	20128	7	92.8	0.75	1.93	0.059	0.0184
103545_at	RIKEN cDNA 2610019E17 gene	EST	75614	17	23.2	0.95	1.92	0.448	0.0573
100982_at	Ngfi-A binding protein 2	Nab2	17937	10	127.7	1.40	1.91	0.009	0.0184
94332_at	E26 avian leukemia oncogene 1, 5' domain	Ets1	23871	9	32.7	0.40	1.88	0.771	0.2077
103063_at	zinc finger protein 62	Zfp62	22720	11	49.8	1.06	1.87	0.244	0.0184
103074_f_	TAF9 RNA pol II, (TBP)-associated factor	Taf9	108143	13	97.0	1.51	1.86	0.302	0.0573
160321_at	zinc finger protein 216	Zfp216	22682	19	20.6	0.74	1.85	0.529	0.0250
102940_at	lymphotoxin B	Ltb	16994	17	33.8	0.90	1.85	0.661	0.0573
100880_at	Mus musculus diabetic nephropathy-relat	---	NA	3	143.2	0.62	1.84	0.639	0.0573
92233_at	RIKEN cDNA 1810007M14 gene	EST	67367	16	91.6	0.80	1.84	0.512	0.0573
101023_f_	RIKEN cDNA 0610010E21 gene	EST	68332	7	21.9	1.71	1.83	0.125	0.0184
101587_at	epoxide hydrolase 1, microsomal	Ephx1	13849	1	181.7	2.15	1.82	0.006	0.0114
93596_i_a	RIKEN cDNA 2410043G19 gene	2410043(	67126	2	176.4	1.49	1.80	0.280	0.0184
96699_at	HMG nucleosomal binding domain 1	Hmgn1	15312	11	105.4	0.69	1.79	0.930	0.0999
98410_at	interferon-g induced GTPase	Gtpi-pend	54396	11	58.85	0.577	1.79	0.013	0.0082
160123_at	RIKEN cDNA 1700008C22 gene	EST	75454	2	25.84	1.143	1.78	0.384	0.0573

C

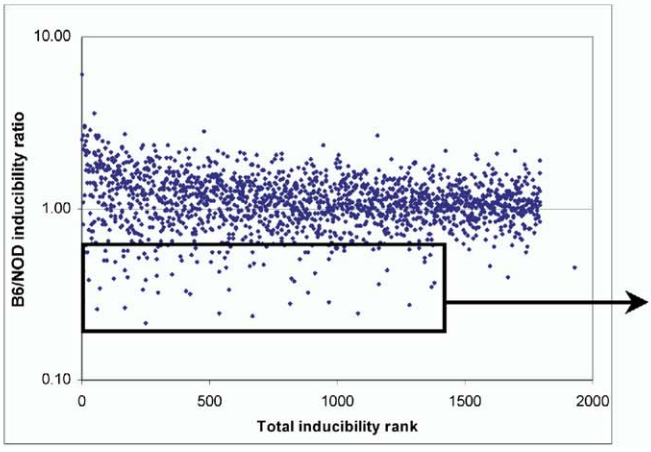

Probe	Title	Symbol	Locus Link	B6/NOD ind. ratio
94332_at	E26 avian leukemia oncogene 1,	Ets1	23871	0.21
104750_a	IFN gamma inducible protein	Irg47	15953	0.24
100981_a	IFN-induced with tetratricopeptid	Ifit1	15957	0.24
160620_a	ROSA 26	ROSA26	14910	0.24
160150_f_	calponin 3, acidic	Cnn3	71994	0.26
94395_at	EST	D3Ertd330e	51886	0.26
97848_at	RNA binding motif, X chromoson	Rbmx	19655	0.27
104070_a	p300/CBP-associated factor	Pcaf	18519	0.28
95024_at	ubiquitin specific protease 18	Ubp43	24110	0.28
103674_f_	eukaryotic translation initiation fa	Eif2s3y	26908	0.29
98509_at	hypothetical protein MGC7434	BC002199	211556	0.32
101422_a	formin binding protein 4	Fnbp4	55935	0.32
98410_at	interferon-g induced GTPase	Gtpi	54396	0.32
96532_at	EST	---	NA	0.33
160933_a	IFN gamma induced GTPase	Igtp	16145	0.33
100880_a	Mus musculus diabetic nephropa	---	NA	0.34
103446_a	interferon induced helicase	Ifih1	71586	0.34
94250_at	eukaryotic translation initiation fa	Eif3s10	13689	0.35
160686_a	EST	5730555F13	66660	0.36
103202_a	guanylate nucleotide binding pro	Gbp3	55932	0.37
161511_f_	interferon-stimulated protein	Isg15	53606	0.38

Figure 5. Distinct Pattern of Gene Induction in BDC2.5/B6g7 and BDC2.5/NOD

(A) Fold induction and ranking for the genes induced more than 1.5-fold in BDC2.5/B6g7 at 16 hr versus 0 hr (red), and their parallel induction for BDC2.5/NOD (blue). Listed are the top 33 genes induced in BDC2.5/B6g7. Induction and repression of more than 1.5-fold are color coded in orange and blue, respectively.

(B) The same plot as in (A) for the genes induced more than 1.5-fold in BDC2.5/NOD (blue) and their fold induction in BDC2.5/B6g7 (red).

(C) The ratio of inducibility (B16/B0 divided by N16/N0) versus inducibility rank. Listed are the top 21 genes ordered by inducibility in NOD versus B6g7.

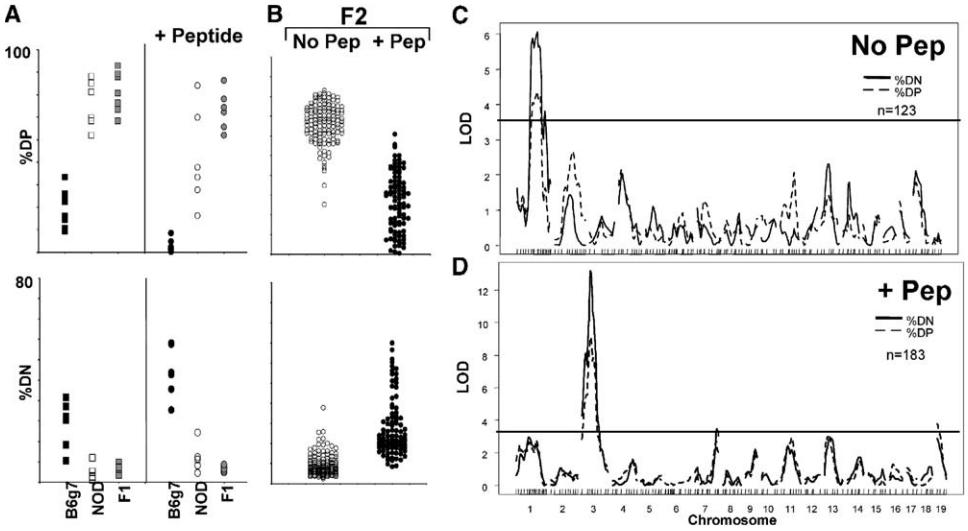

Figure 6. Intervals on *Chr1* and *Chr3* Influence Resistance to Negative Selection

(A) BDC2.5-tg FTOCs were cultured for 7 days without added peptide (squares) or with 10 ng/ml BDCmi (circles) and were analyzed by flow cytometry (compiled from three or more experiments).

(B) Phenotypic distributions for BDC2.5/F2 FTOCs incubated without added peptide (open circles) or with 10 ng/ml BDCmi (filled circles).

(C and D) LOD plots for the (C) no-peptide and (D) plus-peptide FTOC BDC2.5/F2 cohorts.

ent dominance of NOD alleles in the F1, and with the existence of several controlling QTLs.

A genome-wide scan was then performed on genomic DNA from the 306 F2 embryos, genotyped by fluorogenic PCR for a set of 147 SNP markers distinguishing the NOD and B6 genomes. The markers covered all 19 autosomes, in particular known diabetes-linked *Idd* loci, with an average spacing of approximately 16 Mb. Tabulations of the full marker set and of the genotyping results are available as Supplemental Data (Tables S2 and S3). The %DP and %DN values were chosen as the main quantitative traits in this analysis because: a) these metrics most clearly and consistently reflected the differences between NOD and B6g7 FTOCs (Figures 2 and 6A); b) clonal deletion in this instance operates on the DP population, while the DN precursors remain relatively fixed in number; thus, their proportion provides a reasonably robust metric of deletion. We did not track the proportion of CD4-SP cells, a priori a logical choice for an MHC class II-restricted T cell clonotype, because of the additional variability imparted by agonist-induced selection toward the CD8$\alpha\alpha$ lineage. The total cell number per lobe also proved unreliable, as yields in individual FTOCs fluctuate markedly, even when comparing genetically homogeneous embryos.

Simple trait/marker association and interval mapping (S-plus, Mapmaker/QTL, R/qtl) gave rise to very similar results (Figure 6C). For the cultures without peptide addition, which relied on the limited amount of endogenous BDC2.5 Ag to provoke clonal deletion, a major peak was found on *Chr1*, with LOD scores of 4.2 and 5.9 for %DP and %DN QTs, respectively, and accounting for 15.2% of the variance. Permutation tests (R/qtl, 10,000 permutations) established that these peaks were well within the range of significant linkage, with an experiment-wise empirical p value of 0.05 at LOD of 3.49. The NOD allele was fully dominant and was associated with high DP and low DN values, consistent with the NOD phenotype being largely dominant in the F1 (Figure 6A). Lesser linkage peaks, e.g., on *Chr2*, *4*, *13*, and *18*, remained in the "suggestive" range. Thus, resistance to negative selection at low peptide doses potentially maps to multiple loci in the NOD genome, but with a dominant region on *Chr1*.

A different profile was found with the peptide-supplemented F2 cohort, with a major peak on *Chr3* (LOD = 14.2) (Figure 6D), and secondary peaks on *Chr1*, *7*, *11*, and *19*. *Chr3* was calculated to contribute 31.2% of the variance under these conditions. For all of these loci, the NOD allele was again found to be associated with high %DP and low %DN. The divergent profile compared with that of the F2 cohort with no peptide addition indicates that different pathways might be involved: at low levels of deleting signal, a polymorphism (or polymorphisms) on *Chr1* has (have) the principal influence; but, stronger deleting signals, which likely overcome the resistance imparted by *Chr1* loci, unmask the influence of *Chr3*. Interestingly, Sprent and colleagues have reported a similar dichotomy in molecular requirements for clonal deletion of mature thymocytes, differing according to ligand avidity (Kishimoto et al., 1998).

As discussed above, the %DP and %DN values were considered the most useful metrics of clonal deletion. However, we also observed strong evidence for linkage by using %CD8-SP as a QT, independent of clonal deletion. For both the no-peptide and plus-peptide cohorts, a broad peak was observed in the central region of *Chr7* (LOD scores of 4.5 and 4.8, respectively; combined LOD score of 9.69; Figure S2). High %CD8-SP values were associated with the B6 allele in a largely dominant fashion. Its high values did not correlate with

the deletion metrics, and they probably relate to relative commitment to the CD4 versus CD8 lineages (Figure 3 and discussed above), or to thymocyte survival and persistence.

These results were largely confirmed by using a nonparametric interval mapping algorithm in R/qtl and composite interval mapping in Win/QTL Cartographer. Searching for epistatic interactions with two-dimensional scanning in R/qtl yielded suggestive epistatic effects between *Chr1* and *Chr4*, but permutation tests revealed that the evidence for interaction did not meet statistically stringent criteria.

Merging Gene Expression Profiling and Genetic Mapping

The experimental logic behind our parallel gene expression profiling and genetic mapping analyses was that the data sets would crosscomplement, focusing attention on differentially expressed genes or gene families mapping under the genetic linkage peaks. For increased resolution, additional SNPs mapping to the *Chr1* and *Chr3* regions were typed, and confirmatory RT-PCRs were performed for those candidate genes showing suggestive differences in the microarray data. On *Chr1*, the main genetic interval mapped telomeric of the *Idd5* subregions (*ctla4*, *nramp*) that have been shown to influence diverse aspects of peripheral tolerance induction (Sharpe and Freeman, 2002) (Figure 7A). Several genes within this interval did, however, exhibit suggestive microarray profiles (Figure 7B). The first two of these are particularly striking because of their known relevance to apoptosis: PD1 (*pdcd1*, 94 Mb), previously implicated in the control of immune tolerance (Nishimura et al., 1999), was induced 17-fold by addition of the BDCmi peptide in BDC2.5/B6g7 FTOCs, but only 4.8-fold in BDC2.5/NOD cultures. (Confirmatory PCR data for this and other attractive candidates are presented in Figure 7C.) Conversely, the *bcl2*β isoform was upregulated in BDC2.5/NOD relative to BDC2.5/B6g7 cultures. Another gene that could potentially act as a modifier of negative selection is the protein phosphatase *ptprv*, which might modulate TCR signals and was overexpressed in FTOCs of NOD genetic background, prior to and independent of TCR engagement by agonist. In addition, two uncharacterized ESTs were overexpressed in BDC/B6g7.

The associated interval on *Chr3* includes or is flanked by several *Idd* regions (Figure 7A). *Idd3* maps somewhat outside this interval, as do *Idd10* and *Idd18* (Lyons et al., 2000; Lyons et al., 2001), and their likeliest candidates have no obvious connection to the clonal deletion phenotype. On the other hand, the *Idd17* region (80–88 Mb) is included in our *Chr3* interval associated with ineffective clonal deletion (Lyons et al., 2001). As with *Idd3*/*10*/*18*, the *Idd17* interval contains no glaring candidates expected to influence negative selection. We do note the differential induction of *Narg1* ("NMDA receptor-regulated gene 1") (Figure 7B) and *Ash1l*, but it is not clear how these molecules would affect clonal deletion. The *CD1d1* gene makes a more interesting candidate because of its involvement in activation-induced death of peripheral T cells (Dao et al., 2001), as does the *Sh2d2a* gene (aka TSAd, or "lck adaptor critical for cell death"), which lies just outside the published borders of *Idd17*. It is far less induced in BDC2.5/NOD than in BDC2.5/B6g7 FTOCs, and one can speculate that this differential upregulation is at the root of the different transcription programs engaged by agonist on the two genetic backgrounds.

Discussion

The data presented herein confirm and extend, for a TCR/Ag pair involved in spontaneous autoimmunity in the NOD mouse, previous reports demonstrating resistance of NOD thymocytes to clonal deletion triggered by an anti-CD3 mAb (Kishimoto and Sprent, 2001) or by a transgene-encoded neo-self-Ag (Lesage et al., 2002). Because of an intrinsic variation in the interpretation or transmission of signals received through the TCR, immature thymocytes of the NOD genetic background seemed to be far more resistant to death provoked by recognition of self-MHC/Ag complexes. Titration experiments revealed a hundred-fold differential.

In addition to a resistance to clonal deletion, the NOD genome imparts a reduced ability to divert self-reactive thymocytes into an alternative pathway of differentiation that results in T cells of the CD8$\alpha\alpha$ phenotype. As CD8$\alpha\alpha$ thymocytes are precursors of intraepithelial lymphocytes (IELs) (Leishman et al., 2002; and references therein), this aberrancy may lead to a reduced IEL compartment in NOD mice. Thus, the genetic variant(s) underlying the NOD defect in T cell tolerance may impinge at an early point of the signal transduction cascade initiated by engagement of the TCR on thymocytes, upstream of the divergence between apoptosis induction and CD8$\alpha\alpha$ differentiation.

The defects in clonal deletion and diversion likely result in an enrichment for autoreactive specificities in the nascent T cell repertoire of NOD mice, providing an explanation for their propensity to autoimmune disease. However, this is not the only level at which the NOD genome controls the development of autoimmunity or of autoimmune disease. Autoimmunity is also influenced by peripheral tolerance, governing the ability of the autoreactive repertoire to be activated and/or regulated. Different genes or clusters of genes might, to at least some degree, be involved in central and peripheral tolerance phenomena, e.g., the CTLA-4/ICOS family of costimulatory molecules does not seem to be involved in the events described here, mapping to a distinct region of *Chr1*. Overt development of autoimmune disease—in the present context, the insulitis to diabetes conversion—is regulated by still other factors. And herein lies the explanation for why BDC2.5/B6g7 mice actually succumb to type-1 diabetes more rapidly and penetrantly than do BDC2.5/NOD animals (Gonzalez et al., 1997). As recently reported (Poirot et al., 2004), NK cells are powerful regulators of the aggressivity of the insulitic lesion, and the B6 background is associated with a more potent NK cell compartment. The genetic control of autoimmune disease plays a balancing act, and a propensity to poor central tolerance can coexist with stronger peripheral tolerance, possibly, but not necessarily, because of the same polymorphisms.

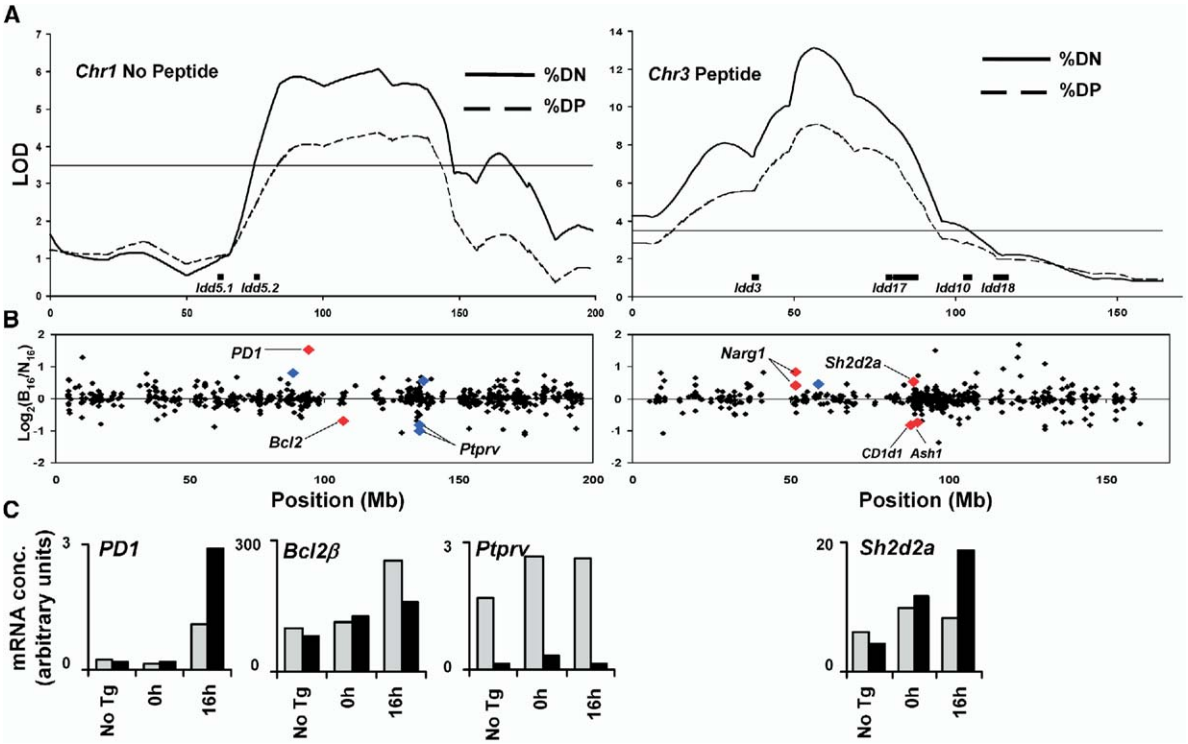

Figure 7. Candidate Genes at the Intersection of Expression Profiling and Genetic Mapping

(A) Linkage maps for *Chr1* (no-peptide cohort) and *Chr3* (plus-peptide cohort). *Idd* regions identified in previous studies are indicated by horizontal bars.

(B) Microarray expression data for all genes represented on the chip for *Chr1* and *Chr3*, presented as the $\log_2$ of the expression ratio for BDC2.5/B6g7 versus BDC2.5/NOD after 16 hr of peptide challenge. Highlighted are genes located within the causal genetic intervals that exhibit bedrock expression differences (blue) or differential induction over time (red). Several genes/ESTs that showed suggestive expression profiles at 16 hr were excluded as candidates for the reasons indicated (Supplemental Data).

(C) Expression data from quantitative RT-PCR (*PD1*, *Ptprv*, *Sh2d2a*) or microarray (*Bcl2β*) analyses of mRNA from sorted FTOC DPs (gray bar, BDC2.5/NOD; black bar, BDC2.5/B6g7).

Even though it is implicit from the experimental setup, which entails the same MHC in both BDC2.5/NOD and BDC2.5/B6g7 mice, one should stress that the resistance to clonal deletion we have explored does not involve the MHC, but other genetic regions. It has been proposed that the NOD MHC class II isoform A^{g7} (and its DQ8 homolog in humans) may predispose to autoimmunity through altering the kinetics/specificity of antigen presentation (reviewed in Nepom and Kwok, 1998). The phenomenon described here operates in addition to any impact the MHC may have on differential selection of autoreactive T cells. Interestingly, the deletion-resistant phenotype imparted by the NOD allele appears dominant, which contrasts with the recessive nature of diabetes susceptibility overall in NOD outcrosses.

Multiple genetic intervals were implicated in the subphenotype we explored, even though a priori it seemed to be a relatively simple one. Different intervals dominated when endogenous antigen was presented at low doses versus when the TCR was more decisively engaged by higher doses of peptide that was exogenously added. Specifically, the *Chr1* interval became less important and the *Chr3* interval took precedence. Such a dichotomy is reminiscent of a previous report that different signaling pathways may come into play during thymocyte deletion at high and low ligand concentrations (Kishimoto et al., 1998). The constellation of loci capable of modulating negative selection that has accumulated in the NOD genome probably reflects the selection pressure applied during the derivation of this inbred strain (Makino et al., 1980). It also suggests that the *Mus* species, as a whole, may benefit from maintaining a pool of genetic variation able to dampen repertoire attrition through negative selection, perhaps to avoid repertoire "holes" for specificities needed to effectively confront microbial challenges.

Genomics

The broad perspective offered by the microarray and PCR analyses revealed two main molecular aspects to the NOD strain's resistance to clonal deletion. First, there was a reduced induction of key molecules of the apoptotic pathway, including *Nur77* and *Bim*. This dampening extended to many other genes as well: those transcripts most strongly induced by clonal deletion triggers on the B6g7 background did show a detectable, but weak, increase on the BDC2.5/NOD background, but the remainder of the response profile was essentially null. Preliminary results suggest that the re-

duction in RNA transcript levels is transcriptional and, at least for the *Nur77* locus, stems from a difference in chromatin accessibility (M. Fassett, D.M., and C.B., unpublished data). A second key facet to the differential response was that BDC2.5/NOD cells engaged a distinct program of transcription. Many of the genes induced in BDC2.5/NOD thymocytes were unaffected, or even repressed, in thymocytes of the B6 background. A preferential induction of the antiapoptotic molecule FLIP after anti-CD3 triggering has been reported for NOD mice vis a vis B6 (Kishimoto and Sprent, 2001), but the present microarray data did not reproduce this difference. Rather, our results indicated that FLIP was one element of a much broader response induced in BDC2.5/NOD thymocytes, including Bcl2 and a number of other survival factors.

The list of genes preferentially induced in BDC2.5/NOD FTOCs is highly suggestive and includes genes involved at three levels of genetic control: transcription, translation, and interferon (IFN)-mediated regulation. The transcription factor Ets-1 promotes T cell survival (reviewed in Sementchenko and Watson, 2000). The RNA splicing factor Rbmx and histone-acetyltransferase Pcaf may regulate broader gene transcription programs. Translational arrest is associated with the induction of apoptosis, in part through inactivation of translation preinitiation complexes (Clemens et al., 2000). Thus, upregulation of *Eif3s10* and *Eif2s3y* is likely to confer resistance to apoptosis in NOD thymocytes. IFN signaling is connected to apoptosis, growth arrest, and cell cycle progression (Stark et al., 1998). A surprisingly high number of inteferon-controlled genes scored in our analysis (7 out of 21). Isg15 is the IFN-inducible member of the ubiquitin-like family of proteins, which modifies IFN signaling by conjugating to multiple target proteins. Ubp43, another IFN-induced protein with deubiquitinase activity, specifically cleaves Isg15 from its target proteins. The presence of two biochemically connected genes in this rather short list points to precise and coordinated regulation of the IFN signaling pathway during clonal deletion. Even more striking is the group of interferon-inducible GTPase (IIGP) family members (Irg47, Gtpi, Igtp, and Gbp3) reported to exert antiapoptotic effects through Akt activation and suppression of Caspase-9 and Caspase-3 (Zhang et al., 2003). In short, then, apoptosis is inhibited in thymocytes of the NOD background through active induction of a broad array of antiapoptotic functions.

Genetics

Intersection of the gene expression profiling and whole-genome screening data highlighted some very attractive candidate genes potentially responsible for the NOD strain's resistance to clonal deletion of self-reactive thymocytes.

bcl2

The classic antiapoptotic gene, *bcl2*, maps to the implicated interval on *Chr1*, and it showed up as upregulated in NOD FTOCs in our genomic analysis. Over- or underexpression of Bcl2 per se has not thus far been tied to thymocyte clonal deletion (Sentman et al., 1991), but it is noteworthy that the B6 versus NOD difference detected in our microarray analysis, and confirmed by RT-PCR, concerned the contribution of splice forms of the transcript rather than overall transcript levels. The existence of Bcl2 splice variants was reported some time ago, but their functional implications remain obscure. There have been recent reports of Bcl2 physically interacting with both Nur77 and Bim (Lin et al., 2004; Zhu et al., 2004), so it is tempting to speculate that an altered ratio of Bcl2 splice forms might influence the proapoptotic activities of Bim/Nur77 through preferential binding of one form or the other. It would be particularly interesting if it were to turn out that the *bcl2* gene follows the precedent of the *ctla4* gene in being controlled by preferential splicing in NOD versus other mouse strains.

pdcd1

The *PD-1* gene (*pdcd1*), whose transcription was markedly underactivated in BDC2.5/NOD FTOCs, maps close to the *bcl2* locus. PD-1 is a member of the CTLA-4/CD28/ICOS family of costimulatory molecules, and its relevance to apoptosis and autoimmunity was established by the phenotype of PD-1-deficient mice, which present with uncontrolled autoreactive lymphocytes (Nishimura et al., 1999) although an impact on negative selection was not demonstrated (Blank et al., 2003). Blockade of PD1 elicited rapid-onset diabetes in NOD mice, consistent with a role in peripheral tolerance pathways (Ansari et al., 2003). Our data suggest that the NOD allele might act as a poorly inducible hypomorph.

ptprv and Tsad

Finally, the *ptprv* and *Tsad* genes (on *Chr1* and *Chr3*, respectively) are interesting candidates, both higher up in the signal transduction pathway. Ptprv, a receptor-type tyrosine phosphatase not thoroughly investigated in the immunological context, was consistently overexpressed in BDC2.5/NOD FTOCs. TSAd (aka Sh2d2a, Lad, RIBP), induced in BDC2.5/B6g7 but not BDC2.5/NOD cultures, is an SH2 adaptor protein that interacts with Lck and Itk at the very apex of TCR-mediated signaling and may have a role as an activating transcription factor. It was previously associated with defective T cell death and autoimmunity (Drappa et al., 2003; Rajagopal et al., 1999). For both the *ptprv* and *Tsad* genes, genetic variation in the basal expression or inducibility could affect the intensity or quality of the signal received through the TCR, in a manner that conditions whether this signal ends up triggering a B6-like program (culminating in the activation of Nur77 and Bim) or a NOD-like program (arriving predominantly at Ets-1 and other survival factors). It may not be just a coincidence that two genes recently found to be associated with type-1 diabetes in humans, those encoding the tyrosine phosphatase PTPN22 and the IκBα modifier SUMO-4, also influence proximal signaling events emanating from the TCR (Bottini et al., 2004; Bohren et al., 2004).

As in the multiorgan autoimmune diseases of aire-deficient mice and AIRE-defective patients, autoimmune diabetes in NOD mice is (at least partially) rooted in a fundamental defect in T cell central tolerance induction, more specifically in clonal deletion of self-reactive thymocytes. Unlike the disease of patients or mice with a mutation in AIRE, wherein autoreactive T cells emerge from the thymus because of a defect in

stromal cell function, the central tolerance deficit we have uncovered in NOD mice is intrinsic to the T cell lineage. Thus, defective T cell central tolerance induction in type-1 diabetes, in NOD mice or in human patients, can be caused by genetic variation at (at least) three levels: because presentation of the autoantigen in the thymus is limiting; because the intracellular channeling of signals emanating from the TCR activates survival rather than apoptosis of thymocytes (through variation in *ptprv* or *PTPN22*, for example); or because of variability in the level of basal expression or inducibility of molecules that control the final pro-/antiapoptotic balance. That the genetic mapping of autoimmune diabetes has been so challenging may not be a surprise in hindsight.

Supplemental Data

Supplemental Data including technical details (Experimental Procedures) are available at http://www.immunity.com/cgi/content/full/22/3/385/DC1/.

Acknowledgments

We thank E. Hyatt and T. Lipatova for help with maintaining the mouse colony, W. Besse and R. Melamed for help with the genotyping and microarray data analysis, G. Losyev for flow cytometric analysis, R. Falcone and the Microrarray Core for chip hybridization, and members of the cbdm diabetes group for inspiring discussion. This work was supported by a grant from the Juvenile Diabetes Research Foundation to D.M. and C.B. (4-2004-368), funds from the William T. Young Chair in Diabetes Research, and Joslin's National Institute of Diabetes and Digestive Kidney Diseases-funded Diabetes and Endocrinology Research Center cores. S.Z. received postdoctoral fellowship support from the American Diabetes Association (Mentor-based Fellowship), P.H. received support from the Cancer Research Institute, and T.Y. received support from the Uehara Memorial Foundation and the Iacocca Foundation.

Received: September 13, 2004
Revised: January 4, 2005
Accepted: January 6, 2005
Published: March 22, 2005

References

Ansari, M., Salama, A.D., Chitnis, T., Smith, R.N., Yagita, H., Akiba, H., Yamazaki, T., Azuma, M., Iwai, H., Khoury, S.J., et al. (2003). The programmed death-1 (PD-1) pathway regulates autoimmune diabetes in nonobese diabetic (NOD) mice. J. Exp. Med. *198*, 63–69.

Apostolou, I., Sarukhan, A., Klein, L., and von Boehmer, H. (2002). Origin of regulatory T cells with known specificity for antigen. Nat. Immunol. *3*, 756–763.

Bergman, B., and Haskins, K. (1994). Islet-specific T-cell clones from the NOD mouse respond to beta-granule antigen. Diabetes *43*, 197–203.

Blank, C., Brown, I., Marks, R., Nishimura, H., Honjo, T., and Gajewski, T.F. (2003). Absence of programmed death receptor 1 alters thymic development and enhances generation of CD4/CD8 double-negative TCR-transgenic T cells. J. Immunol. *171*, 4574–4581.

Bohren, K.M., Nadkarni, V., Song, J.H., Gabbay, K.H., and Owerbach, D. (2004). A M55V polymorphism in a novel SUMO gene (SUMO-4) differentially activates heat shock transcription factors and is associated with susceptibility to type I diabetes mellitus. J. Biol. Chem. *279*, 27233–27238.

Bottini, N., Musumeci, L., Alonso, A., Rahmouni, S., Nika, K., Rostamkhani, M., MacMurray, J., Meloni, G.F., Lucarelli, P., Pellecchia, M., et al. (2004). A functional variant of lymphoid tyrosine phosphatase is associated with type I diabetes. Nat. Genet. *36*, 337–338.

Bouillet, P., Purton, J.F., Godfrey, D.I., Zhang, L.C., Coultas, L., Puthalakath, H., Pellegrini, M., Cory, S., Adams, J.M., and Strasser, A. (2002). BH3-only Bcl-2 family member Bim is required for apoptosis of autoreactive thymocytes. Nature *415*, 922–926.

Calnan, B.J., Szychowski, S., Chan, F.K., Cado, D., and Winoto, A. (1995). A role for the orphan steroid receptor Nur 77 in apoptosis accompanying antigen-induced negative selection. Immunity *3*, 273–282.

Clemens, M.J., Bushell, M., Jeffrey, I.W., Pain, V.M., and Morley, S.J. (2000). Translation initiation factor modifications and the regulation of protein synthesis in apoptotic cells. Cell Death Differ. *7*, 603–615.

Dao, T., Exley, M., Mehal, W.Z., Tahir, S.M., Snapper, S., Taniguchi, M., Balk, S.P., and Crispe, I.N. (2001). Involvement of CD1 in peripheral deletion of T lymphocytes is independent of NK T cells. J. Immunol. *166*, 3090–3097.

DeRyckere, D., Mann, D.L., and DeGregori, J. (2003). Characterization of transcriptional regulation during negative selection in vivo. J. Immunol. *171*, 802–811.

Drappa, J., Kamen, L.A., Chan, E., Georgiev, M., Ashany, D., Marti, F., and King, P.D. (2003). Impaired T cell death and lupus-like autoimmunity in T cell-specific adapter protein-deficient mice. J. Exp. Med. *198*, 809–821.

Fiorini, E., Schmitz, I., Marissen, W.E., Osborn, S.L., Touma, M., Sasada, T., Reche, P.A., Tibaldi, E.V., Hussey, R.E., Kruisbeek, A.M., et al. (2002). Peptide-induced negative selection of thymocytes activates transcription of an NF-kappa B inhibitor. Mol. Cell *9*, 637–648.

Gonzalez, A., Katz, J.D., Mattei, M.G., Kikutani, H., Benoist, C., and Mathis, D. (1997). Genetic control of diabetes progression. Immunity *7*, 873–883.

Huang, Y.H., Li, D., Winoto, A., and Robey, E.A. (2004). Distinct transcriptional programs in thymocytes responding to T cell receptor, Notch, and positive selection signals. Proc. Natl. Acad. Sci. USA *101*, 4936–4941.

Jordan, M.S., Boesteanu, A., Reed, A.J., Petrone, A.L., Holenbeck, A.E., Lerman, M.A., Naji, A., and Caton, A.J. (2001). Thymic selection of CD4+CD25+ regulatory T cells induced by an agonist self-peptide. Nat. Immunol. *2*, 283–284.

Judkowski, V., Pinilla, C., Schroder, K., Tucker, L., Sarvetnick, N., and Wilson, D.B. (2001). Identification of MHC class II-restricted peptide ligands, including a glutamic acid decarboxylase 65 sequence, that stimulate diabetogenic T cells from transgenic BDC2.5 nonobese diabetic mice. J. Immunol. *166*, 908–917.

Kanagawa, O., Militech, A., and Vaupel, B.A. (2002). Regulation of diabetes development by regulatory T cells in pancreatic islet antigen-specific TCR transgenic nonobese diabetic mice. J. Immunol. *168*, 6159–6164.

Katz, J.D., Wang, B., Haskins, K., Benoist, C., and Mathis, D. (1993). Following a diabetogenic T cell from genesis through pathogenesis. Cell *74*, 1089–1100.

Kishimoto, H., and Sprent, J. (2001). A defect in central tolerance in NOD mice. Nat. Immunol. *2*, 1025–1031.

Kishimoto, H., Surh, C.D., and Sprent, J. (1998). A role for Fas in negative selection of thymocytes in vivo. J. Exp. Med. *187*, 1427–1438.

Kyewski, B., Derbinski, J., Gotter, J., and Klein, L. (2002). Promiscuous gene expression and central T-cell tolerance: more than meets the eye. Trends Immunol. *23*, 364–371.

Leishman, A.J., Gapin, L., Capone, M., Palmer, E., MacDonald, H.R., Kronenberg, M., and Cheroutre, H. (2002). Precursors of functional MHC class I- or class II-restricted CD8alphaalpha(+) T cells are positively selected in the thymus by agonist self-peptides. Immunity *16*, 355–364.

Lesage, S., Hartley, S.B., Akkaraju, S., Wilson, J., Townsend, M., and Goodnow, C.C. (2002). Failure to censor forbidden clones of CD4 T cells in autoimmune diabetes. J. Exp. Med. *196*, 1175–1188.

Lin, B., Kolluri, S.K., Lin, F., Liu, W., Han, Y.H., Cao, X., Dawson,

M.I., Reed, J.C., and Zhang, X.K. (2004). Conversion of Bcl-2 from protector to killer by interaction with nuclear orphan receptor Nur77/TR3. Cell *116*, 527–540.

Lyons, P.A., Armitage, N., Argentina, F., Denny, P., Hill, N.J., Lord, C.J., Wilusz, M.B., Peterson, L.B., Wicker, L.S., and Todd, J.A. (2000). Congenic mapping of the type 1 diabetes locus, Idd3, to a 780-kb region of mouse chromosome 3: identification of a candidate segment of ancestral DNA by haplotype mapping. Genome Res. *10*, 446–453.

Lyons, P.A., Armitage, N., Lord, C.J., Phillips, M.S., Todd, J.A., Peterson, L.B., and Wicker, L.S. (2001). Mapping by genetic interaction: high-resolution congenic mapping of the type 1 diabetes loci Idd10 and Idd18 in the NOD mouse. Diabetes *50*, 2633–2637.

Makino, S., Kunimoto, K., Muraoka, Y., Mizushima, Y.K.K., and Tochino, Y. (1980). Breeding of a non-obese, diabetic strain of mice. Exp. Anim. *29*, 1–6.

Nepom, G.T., and Kwok, W.W. (1998). Molecular basis for HLA-DQ associations with IDDM. Diabetes *47*, 1177–1184.

Nishimura, H., Nose, M., Hiai, H., Minato, N., and Honjo, T. (1999). Development of lupus-like autoimmune diseases by disruption of the PD-1 gene encoding an ITIM motif-carrying immunoreceptor. Immunity *11*, 141–151.

Poirot, L., Benoist, C., and Mathis, D. (2004). Natural killer cells distinguish innocuous and destructive forms of pancreatic islet autoimmunity. Proc. Natl. Acad. Sci. USA *101*, 8102–8107.

Pugliese, A., and Miceli, D. (2002). The insulin gene in diabetes. Diabetes Metab. Res. Rev. *18*, 13–25.

Rajagopal, K., Sommers, C.L., Decker, D.C., Mitchell, E.O., Korthauer, U., Sperling, A.I., Kozak, C.A., Love, P.E., and Bluestone, J.A. (1999). RIBP, a novel Rlk/Txk- and itk-binding adaptor protein that regulates T cell activation. J. Exp. Med. *190*, 1657–1668.

Rathmell, J.C., Lindsten, T., Zong, W.X., Cinalli, R.M., and Thompson, C.B. (2002). Deficiency in Bak and Bax pertubs thymic selection and lymphoid homeostasis. Nat. Immunol. *3*, 932–939.

Schmitz, I., Clayton, L.K., and Reinherz, E.L. (2003). Gene expression analysis of thymocyte selection in vivo. Int. Immunol. *15*, 1237–1248.

Sementchenko, V.I., and Watson, D.K. (2000). Ets target genes: past, present and future. Oncogene *19*, 6533–6548.

Sentman, C.L., Shutter, J.R., Hockenbery, D., Kanagawa, O., and Korsmeyer, S.J. (1991). bcl-2 inhibits multiple forms of apoptosis but not negative selection in thymocytes. Cell *67*, 879–888.

Sharpe, A.H., and Freeman, G.J. (2002). The B7–CD28 superfamily. Nat. Rev. Immunol. *2*, 116–126.

Stark, G.R., Kerr, I.M., Williams, B.R., Silverman, R.H., and Schreiber, R.D. (1998). How cells respond to interferons. Annu. Rev. Biochem. *67*, 227–264.

Starr, T.K., Jameson, S.C., and Hogquist, K.A. (2003). Positive and negative selection of T cells. Annu. Rev. Immunol. *21*, 139–176.

Thebault-Baumont, K., Dubois-Laforgue, D., Krief, P., Briand, J.P., Halbout, P., Vallon-Geoffroy, K., Morin, J., Laloux, V., Lehuen, A., Carel, J.C., et al. (2003). Acceleration of type 1 diabetes mellitus in proinsulin 2-deficient NOD mice. J. Clin. Invest. *111*, 851–857.

Villunger, A., Marsden, V.S., and Strasser, A. (2003). Efficient T cell receptor-mediated apoptosis in nonobese diabetic mouse thymocytes. Nat. Immunol. *4*, 717–718.

Woronicz, J.D., Calnan, B., Ngo, V., and Winoto, A. (1994). Requirement for the orphan steroid receptor Nur77 in apoptosis of T-cell hybridomas. Nature *367*, 277–281.

Yamagata, T., Mathis, D., and Benoist, C. (2004). Self-reactivity in thymic double-positive cells commits cells to a CD8 alpha alpha lineage with characteristics of innate immune cells. Nat. Immunol. *5*, 597–605.

Yamashiro, H., Hozumi, N., and Nakano, N. (2002). Development of CD25(+) T cells secreting transforming growth factor-beta1 by altered peptide ligands expressed as self-antigens. Int. Immunol. *14*, 857–865.

Zhang, Z.L., Constantinou, D., Mandel, T.E., and Georgiou, H.M. (1994). Lymphocyte subsets in thymus and peripheral lymphoid tissues of aging and diabetic NOD mice. Autoimmunity *17*, 41–48.

Zhang, H.M., Yuan, J., Cheung, P., Luo, H., Yanagawa, B., Chau, D., Stephan-Tozy, N., Wong, B.W., Zhang, J., Wilson, J.E., et al. (2003). Overexpression of interferon-gamma-inducible GTPase inhibits coxsackievirus B3-induced apoptosis through the activation of the phosphatidylinositol 3-kinase/Akt pathway and inhibition of viral replication. J. Biol. Chem. *278*, 33011–33019.

Zhu, Y., Swanson, B.J., Wang, M., Hildeman, D.A., Schaefer, B.C., Liu, X., Suzuki, H., Mihara, K., Kappler, J., and Marrack, P. (2004). Constitutive association of the proapoptotic protein Bim with Bcl-2-related proteins on mitochondria in T cells. Proc. Natl. Acad. Sci. USA *101*, 7681–7686.

Accession Numbers

The microarray data GEO accession number is GSE2128.